Andrea Tomalini
Arch. and Ph.D. Student in "Architectural and Landscape Heritage". In 2019 he graduated with honours in Architecture at Politecnico di Torino, he is specializing in digital acquisitions and information modelling. His interests are related to the disciplines of drawing, survey and digital representation of architecture with attention to the use of BIM and VPL methodologies for the management of existing assets.

Edoardo Pristeri
M.Sc. degree in ICT for Smart Societies in 2019 from Politecnico di Torino. He subsequently joined in December 2019 the Photonics & Wireless Solutions, now Connected Systems and Cybersecurity, research group at LINKS Foundation as a Researcher. He is involved in different regional, industrial and European projects and is currently managing activities involving the applications of Machine Learning techniques in the Industry 4.0 scenario.

Jacopo Bono
Ph.D. student in "Architectural and Landscape Heritage". In 2021 he graduated with honors in Architecture (ACC) from the Politecnico di Torino. During his postgraduate period, he won two research scholarships focus on drawing, virtualization, digitization of Heritage. His research interests concern modeling in the H-BIM environment by investigating the construction of parametric and non-standardized libraries.

Tools development to optimize the use of micro-UAS for Architectural Survey

In view of the increasingly widespread use of inoffensive UAS for photogrammetric acquisitions in the architectural and infrastructural spheres, there is a need to be able to program flight missions suited to the operator's needs. This contribution presents the results of two experiments conducted by the research group. The first proposed procedure, based on low-cost instrumentation and algorithms in a VPL environment, fills the gap of proprietary applications and allows the coding and customisation of flight missions for photogrammetry. Obtaining this information is not always easy; immovable or unforeseen obstacles lead to lengthy post-production of the photogrammetric cloud to remove them. The second procedure, by constructing an object segmentation framework, fills this gap by automatically processing photogrammetric images by recreating masks that remove unwanted objects from the dense cloud calculation. Despite some shortcomings, the results are promising and manage to make up for these shortcomings, at least in part.

INTRODUCTION

In recent years, the commercialisation of Un-manned Aerial Systems (UAS) equipped with digital cameras at prices affordable to the general public has enabled the development of new lines of research. Despite the numerous advantages, there are some criticalities sometimes dictated by the complexity of these technologies, or failures, or even results from particularly stringent regulatory constraints. The architectural acquisition offers various possibilities of use and constitutes not only a procedure but a study process that includes the identification of correct methodologies depending on the type of information to be obtained. As far as the documentation of cultural heritage is concerned, we see the increasingly refined integration of different acquisition methodologies. In this context UAS systems certainly play a central role (Lo Brutto et al., 2014).

The contribution proposes the construction of two different software applications:

- The first one plans the optimal flight path, with respective waypoints, to acquire a given Architectural Heritage. The automation of this process aims to decrease gross errors on the part of the pilot. On the other hand, the operator is in no way replaced by these systems. After programming, his task is to monitor the UAS to intervene manually if necessary.
- The second processes the sets of images acquired during the flight and removes the elements that, framed unintentionally, do not help the photogrammetric restitution of the asset and could be a source of the noise.

The proposed methodologies exploit the potential of micro-drones, which are simpler to use at a regulatory level, and aim to optimize field acquisition and post-production times of the collected data, reducing human errors during the survey campaign.

The paper is divided into: an introduction on the explanation of the formulas and calculation of photogrammetric captures; a regulatory summary on the use of UAS in Italy; an identification of the hardware instrumentation used; a description of the acquisition methodology and the algorithm that calculates the mission path; a description of the individual missions and a comment on their execution; introduction to object segmentation and the MASK R-CNN framework; description of the training dataset and integrated restitution methodology; conclusions.

INTRODUCTION TO PHOTOGRAMMETRY SURVEY

Photogrammetry is the technique that allows one to graphically represent, at the desired scale, the shape of an "object" of which one has two photographs, taken from two different points and of known position with respect to it.

In the face of this definition, as stated by De Luca, the application, experimentation, and development of photogrammetry in the field of knowledge of existing architectural reality cannot be surprising (De Luca, 2011); especially in the last few years, since a new union between image-based techniques (Photogrammetry) and the new generation of software (Computer vision) has been established (Aicardi, 2018). Specifically, thanks to a recent bibliometric study by Carmen Marín-Buzón, it is from 2010 that scientific research has increased in literature around photogrammetry. This increase is due to the lowest common denominator of this contribution, the commercialization of unmanned aerial vehicles (UAS) (Marin-Buzòn, 2021). In the face of all this, it is essential to take the discussion back to its origins, focusing on the main parameters to be taken into account to achieve a proper photogrammetric take: the take distance and the longitudinal and transverse overlay.

For a correct photogrammetric take, drawing up a take path is indispensable to have good photographic coverage. The main parameters to be considered are the take distance and the longitudinal and transversal coverage.

Concerning the grasping distance from the subject to be surveyed, it directly depends on the accuracy and scale to be achieved in the restitution phase. Considering the surface to be acquired through a nadiral grasping scheme there is a re-
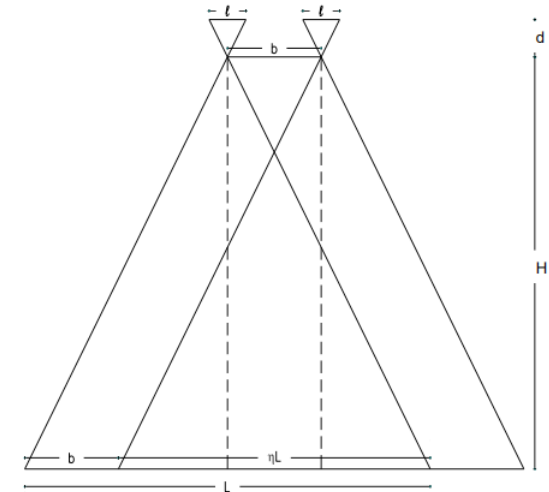

Fig. 1 - Diagram of the geometric relations of nadiral UAS photogrammetry of two consecutive frames with decomposition and identification of the main parameters:
d = Focal lenght
H = Flight height
l = Film - Focal plane - Sensor dimension (230 mm)
L =Area covered
b = Air base - interaxes
nL = Overlap

Formula 1: Ratio between main camera distance and flight altitude; frame format and embrace; frame scale.

$$\frac{1}{N} = \frac{l}{L} = \frac{1}{n}$$

lationship that links the grasping distance from the subject (H), with the main distance (d) of the camera, the camera format (l) and the embrace of the photographed portion of the subject (L) (Fig. 1). This relationship represents the average scale of the frame (1/n).

(d/H)=l/L=1/n (Formula 1).

Regarding the grasping path, the proportions of the object must be taken into account, which is usually made parallel to the largest dimension of the area to be photographed to reduce the number of steps and the transverse and longitudinal coverage of each frame. These parameters can also be entered into a formula to obtain the number of useful frames for a given capture to be distributed evenly along the grip path

REGULATORY BACKGROUND IN ITALY FOR UAS USE

In Italy, the flight of UAS is regulated by the National Civil Aviation Authority (ENAC), which as of 1 January 2021 had to bring Italian regulations into line with European rules dictated by the European Union Aviation Safety Agency (EASA).

EASA has developed, at the request of the European Commission of the member states (27 countries) and other interested parties (Iceland, Liechtenstein, Norway and Switzerland), a common regulatory framework to ensure the correct and free movement of drones within the European Union. The latest documents attempting to achieve this goal are EU Regulations 947/2019 and 945/2019 introduced on 31 December 2020. Specifically, Regulation 947/2019 applies the highest standards achieved in the aviation sector to UAS, in terms of pilot and citizen safety, privacy and overall environmental conditions.

Furthermore, the document summarizes the main operations, performed by the UAS, in three categories: (i) open, represents operations with a low level of risk, therefore no authorisations by the competent authority and/or declarations by the operator are required. This category is subdivided into three subcategories (A1, A2 and A3); (ii) specific, the risk level is moderate, and a distinction is made between standard scenarios (STS) in which

the operator's declaration or possession of LUC certification is required, and not in which authorisation by the authorities is required; (iii) certified in which the pilot must be in possession of certification and the operator must be approved by the authorities. Finally, drone traffic management will be ensured through the drafting of a further EU regulation called U-space[1], published in April 2021(Civil Drones (Unmanned Aircraft), s.d.).

With the new Implementing Regulation (EU) 2019/947, the previous national regulations on UAS operation lapse. ENAC published the UAS-IT Regulation on 4 January 2021, which regulates the competencies to be faced by the Italian State. The ENAC Regulation supplements the European legal framework and specifies the main provisions for pilotage. In this context, it defines the importance of registering one's UAS on the D-Flight portal[2] and affixing the QR identification code to the drone. Furthermore, through the portal, it is possible to apply for the necessary authorisations according to the individual requirements dealt with in the EASA regulations (THE EU DRONE POLICY, s.d.).

Within this new regulation, there is no longer a distinction between hobby and professional use, the factors that matter are: what type of operation is being carried out and what kind of drone is being used. The type of operation, as suggested by the EASA regulations, is distinguished into Open, Specific and Certified. The Open category refers to low-risk operations and it is only possible to operate with your UAS if: the pilot has the certificate issued by ENAC; the UAS operator has registered on the d-flight portal; adequate insurance has been taken out; the cone allowed/banned to fly has been checked on the d-flight portal.

In the Open category, the Maximum Take-Off Mass (MTOM) permitted is 25kg, it is only possible to fly the drone in Visual Line Of Sight (VLOS) mode, a maximum height from the take-off point of 120 m is permitted, and CE marking is mandatory. This category, the one in which we usually operate for photogrammetric acquisitions, is divided into different sub-categories based on the drone's position to people (excluding the pilot) and the MTOM: A1, it is possible to fly over people; A2, close to

people; A3, far from people. It should be noted that in the case of UAS with a MTOM weight of less than 250 g equipped with a camera, it is not compulsory to obtain the certificate and they are considered intrinsically harmless; consequently, it is also possible to fly in built-up areas in compliance with any limitations on the D-flight.it portal and it is not necessary to possess the Operations Manual.

UAS USED

Within the consumer UAS market, those considered harmless and can operate in the Open category are not numerous. Moreover, even fewer of those with an integrated camera with suitable sensor size and focal length. These include DJI's mini-series drones, the Autel EVO nano, and the FIMI X8 Mini. A DJI mini SE was used to test the methods that will be proposed below. The UAS mentioned is a quadricopter with a camera with a 1/2.3" CMOS sensor, a lens equivalent to 35mm:24mm and returns images in 4:3 format of 4000x3000 pixels.

METHODOLOGY FOR FLIGHT PLANNING AND FLIGHT

Three flight modes have been identified in the bibliography (Nex & Remondino, 2014): the first case of manual flight with correctly oriented images; the second case in which the flight is carried out manually and the overlap between the frames is disordered; the third case in which the flight is programmed and the drone can take the images autonomously to have the correct overlap between the frames.

As far as the drone used is concerned, it is impossible to programme a flight path within the manufacturer's application to carry out correct photogrammetry (this shortcoming can be generalized to all the models mentioned above).

To overcome this problem, other developers have proposed applications that allow the flight of the UAS to be programmed. These applications include Litchi, Rainbow, Drone Harmony, Pix4Dcapture, PIX4Dscan, Dronelink and DroneDeploy. The limitation of these applications, besides the fact that

they do not support all UAS models (drones under 250g are often missing), is that the programming of the capture path has few customisation parameters. Having identified the area's perimeter to be captured, it is possible to set the cruising altitude and, in some apps, to set the desired overlap between the various shots. More advanced functions are only available for a fee (often with subscription services), among which one feels the lack of a setting for: the definition of the scale of the final print; the scheduling of the flight to acquire an elevation; the insertion of coordinates around which to have more shots for a more solid cloud.

The proposed methodology relies on low-cost applications that, through algorithms written with Visual Programming Languages (VPL), allow the operator to develop the flight mission suited to his needs. The advantages of this particular procedure are: the possibility of programming missions to acquire vertical surfaces; having full control over each step (control that is not always allowed with third-party apps); unlimited mission customisation possibilities.
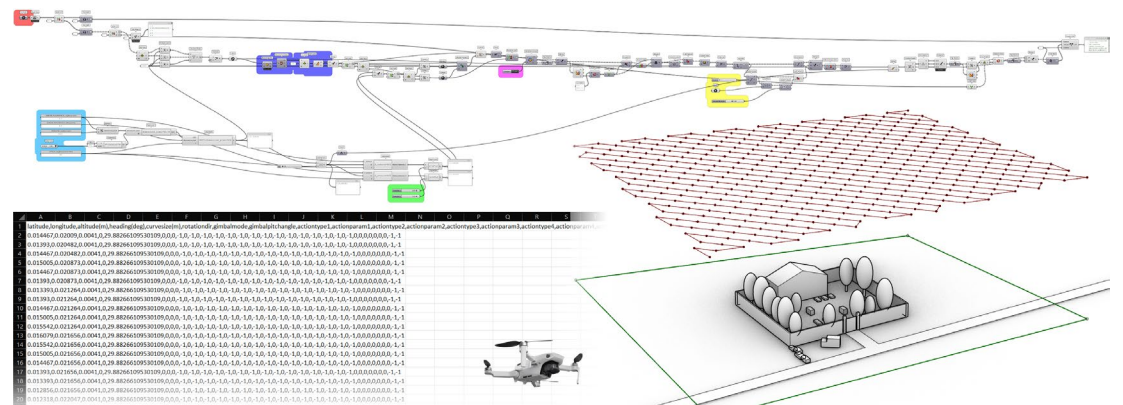
To perform this test, we relied on the Litchi application which, although not a photogrammetry app, is an excellent flight control app in that although DJI does not develop it, it is nevertheless recommended by the manufacturers themselves as an alternative to their original application (ARS, 2021); ; it has a protocol for programming, exporting and importing flight missions in CSV and KML format; associated with the application there is a web page where it is possible to programme the mission (as it is not an app for photogrammetry, the drawing modes are very limited) and preview the programmed route; finally, there is an online guide for programming the actions that can be performed by the drone (in CSV format certain numbers have an associated action -1: no action; 0: Stay For; 1: Take Photo; 2: Start Recording; 3: Stop Recording; 4: Rotate aircraft; 5: Tilt Camera). The workflow consists of three steps: identification of the area to be surveyed and export of the coordinates; construction of the flight path according to the scale of representation, drone specifications and requirements; export of the flight mission and

import of the same into the flight app.

The first step can be performed either on the earth.google application or on the flylitchi.com/hub portal. In both cases, it is necessary to demarcate the area of interest by identifying no less than three placeholders, after which the geospatial data must be downloaded either in KML or CSV format.

The second step is structured in the Grasshopper programming environment (Fig. 2). The algorithm has two sets of inputs: the first is derived from the equipment being used and the scale of representation to be achieved; the second is derived from the geospatial data just downloaded. For the correct functioning of this script, it is essential to enter the data concerning the photographic sensor mounted on our UAS (Width and Height in mm), the dimensions of the images to be taken (Height and Width in pixels) and the focal length of the optics (also expressed in mm). Through the systematization of these data and the indication of the scale, it is possible to calculate the GSD and, consequently, the ground flight altitude not to be exceeded. Extrapolation of the geospatial data and their conversion from the EPSG:3857 - WGS 84 system to an XYZ system makes it possible to measure the area to be acquired and consequently calculate the horizontal and vertical overlap. By setting a percentage of overlap between the

frames, the number of swipes to be made and the number of frames for each swipe are indicated.

The points saved on the CSV or KML file are converted into XYZ type coordinates, indicating the perimeter of the area of interest. The resulting contour polyline (component: PolyLine) is used to find the minimum rectangle that contains it (component: BoundingBox); from this rectangle the direction of the swipes (with respect to the longest side to save time and battery power during the acquisition phase) is determined (component: Dimensions, SortList). The domain of the rectangle is divided in one direction by the number of swipes and in the other by the number of frames (component: Divide Domain^2, Isotrim). Only those portions of the surface's center that are within the initial perimeter are retained (component: Point In Curve, Cull Pattern). The remaining points that correspond to the waypoints required for acquisition are converted from XYZ coordinates to EPSG:3857 - WGS 84. The data obtained are interlaced with the actions to be performed during the flight (component: Text Join). The list of data

Fig. 2 - in the algorithm (upper part of the image) you can see the CSV reading point (highlighted in red), the data relating to the drone camera (highlighted in blue), the overlapping settings (highlighted in green), definition of the direction streaks (highlighted in purple and magenta). Below is an extract of the generated CSV file and the path of the drone.

thus collected is exported and saved in CSV format (component: Panel).

The final step in the process is to upload the CSV file to the mobile phone that will be connected to the radio control of the quadricopter and, once the Litchi app is open and the drone is connected to the radio control, it will be sufficient to open the CSV file and start the mission.

The process simplified in this way can be enriched with various functions, for example, at a specific place of interest, waypoints can be added in which the drone can orient itself in the direction of the place of interest and the gimbal changes inclination before taking the shot (Fig. 3). This enrichment increases the drone's flight time, which performs more actions in a single flight, but decreases the total acquisition time by reducing the timing of take-off, positioning of the device and landing.

This algorithm, if structured differently, can also be used for façade surveying (Fig. 4). The input data is always the same, and placeholders must be positioned around the building to be acquired. Starting from the minimum rectangle containing

Fig 3 - from left, extract of the CSV and visualization of the drone path and direction of the gimabl

Fig 4 - updated algorithm to survey the facades. In the area highlighted in yellow, the route is recalculated on those elevations that have obstacles that hinder the flight of the drone (at the bottom right you can see how it is recalculated around the tree). The bottom left represents the direction in which the shots are taken.

the building, this is extruded (component: Extrude) to a value greater than the building itself. The resulting surfaces are analyzed individually, and the relationship between the height and width of the surface is analyzed (component: Deconstruct Brep, Dimensions). For this type of flight, it was essential to foresee possible obstacles (trees, lampposts, boundary walls, etc.), these are considered as parallelepipeds and the waypoints within them are excluded from the path (component: Point In Breps, Cull Pattern). If there is an obstacle in the path it is split into two parts; The algorithm reconstructs the edges of the pattern that is broken by the obstacle and stitches the two polylines together (component: Join Curves). The export is always the same.

MISSION CONDUCT AND COMMENTARY

To test the automatic flight modes and safely verify their limits, the research team went to a location free of obstacles or crowds of people. The small cemetery of Borgo Cornalese, in the province of Turin, met these requirements. The area acquired comprises the graveyard and a portion of surrounding land enclosed in a rectangle measuring approximately 120m x 80m.

Three different flight missions were carried out at the survey site: the first was a mission during which the drone took 254 images at an altitude of approximately 21 meters with the camera locked

in a position perpendicular to the ground (Fig. 5); the second mission involved a flight altitude of approximately 31 meters above the ground, and the orientation of the drone and the camera had been previously calculated within the algorithm so that they would have the cross placed in a barycentric position at the cemetery as the central point of each frame, 35 frames were acquired the third mission was programmed on site after evaluating obstacles and the portion to be acquired, the shots were programmed to capture a part of the perimeter wall adjacent to the cemetery entrance, 12 frames were acquired.

To carry out the mission, upload the flight file in CSV format to the mission hub and then log in to the device that will be connected to the quadricopter's remote control. Entering the waypoint section displays the saved missions, and you can start from there. The drone takes off and is positioned at the designated altitude, then, leaving the default values, heads to waypoint 1 and the series of shots begins. Although the GPS on board the drone has a vertical accuracy range of +-0.5 m and a horizontal accuracy range of +- 1.5 m, the shots are positioned evenly over the entire area, and the longitudinal and transverse overlap values set during the planning phase are respected. The algorithm showed one of its limitations, it does not take into account the flight time to complete the mission; for this first series of images it was necessary to replace the drone's battery halfway through the
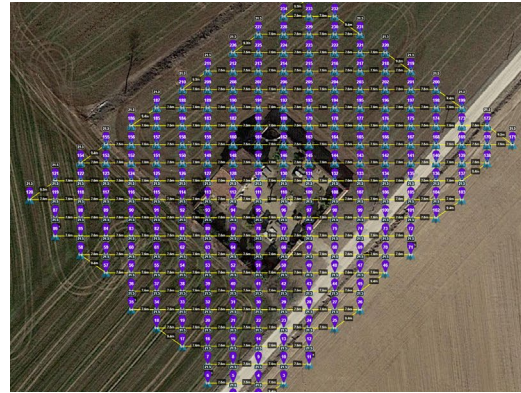
Fig. 5 - First mission. On the left, mission imported to the Litchi app; on the right, alignment of the shots in Agisoft Metashape and representation of each point by means of a reliability gradient.
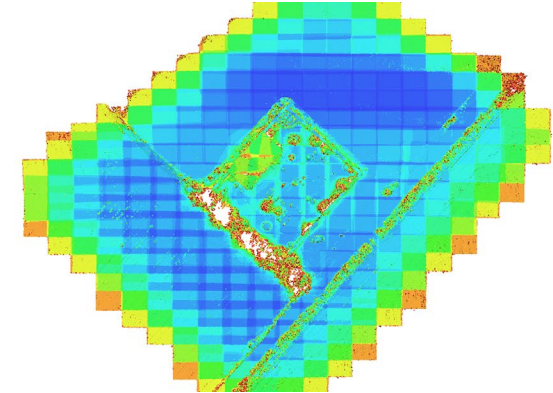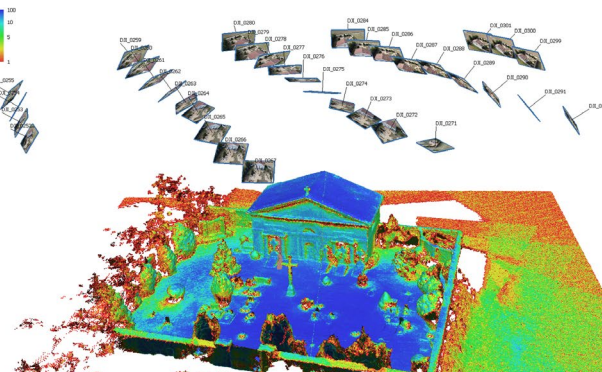

Fig. 6 - Second mission. On the left, mission imported to the Litchi app; on the right, alignment of the shots in Agisoft Metashape and representation of each point by means of a reliability gradient.

mission. Fortunately, within the Litchi app, it is possible to change the mission start waypoint and so it was possible to acquire the missing portion.

The second series of shots (Fig. 6), which was much shorter than the previous one, had no hitches and the positioning of the drone and the camera's rotation with respect to the subject was done correctly without operator intervention.

This third series of shots (Fig. 7) is aimed at evaluating the algorithm's potential for creating patterns that capture vertical portions. In this case, it was decided to take only a few photos as, being the first test, we were not sure whether the script worked adequately (the flight altitude for the first 4 frames was very low and the risk of causing damage to the quadricopter had to be considered). Again despite the hardware limitations of the quadricopter's sensors, the shots were taken successfully, with respect to the position of the shots, it can be seen that the upper crawls are shifted compared to the first set of photographs (the weather conditions could cause the error, since then the wind has been stronger).

In all three cases, the photos were processed with Agisoft Metashape photogrammetry software through a desktop computer with an 11th Gen Intel(R) Core(TM) processor, 64 GB RAM and NVIDIA GeForce RTX 3070 video card (Fig. 8). Starting with an initial phase of photo alignment for each of the three missions, a scattered cloud was generated, resulting from the alignment of the photos, with

the respective points: 371,353 (254 images), 66,890 (35 images) and 8,996 (22 images). The next step was based on the estimated shooting positions of construction of the following dense clouds at medium quality: 14,334,812 (254 images), 2,968,052 (35 images) and 1,290,466 (22 images). In conclusion, the results show how both of the three missions could achieve the correct positioning of the UAS during the taking process and appropriate overlapping of the frames.

INTRODUCTION TO MASK R-CNN AND OBJECT SEGMENTATION

Regarding object detection and segmentation, Mask R-CNN (He et al., 2018) represents one of the solutions developed in recent years to be considered. Object segmentation consists of three main actions: (i) the localisation of the object on the image, (ii) its relative classification and finally, (iii) the generation of the object segmentation mask. Approaches before the introduction of convolutional neural networks had the disadvantage of requiring (i) a large demand in terms of computational capacity and (ii) the need to possess an articulated and complex process consisting of multiple steps.
R-CNN (Girshick et al., 2014), proposed in 2014 by Girshick et al., attempts to solve the region selection problem for object identification in traditional type neural networks. Mask R-CNN can be
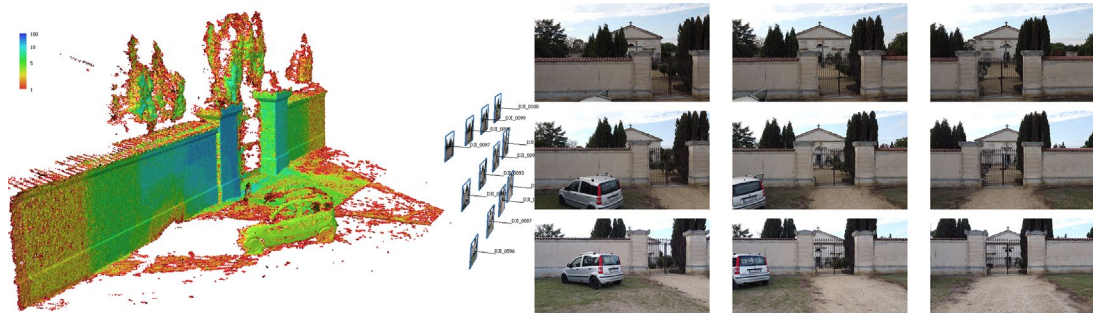

Fig. 7 - Third mission. On the left, alignment of the shots in Agisoft Metashape and representation of each point by means of a reliability gradient. On the right, some frames in which there is an obstacle that generates unwanted portions of the cloud.
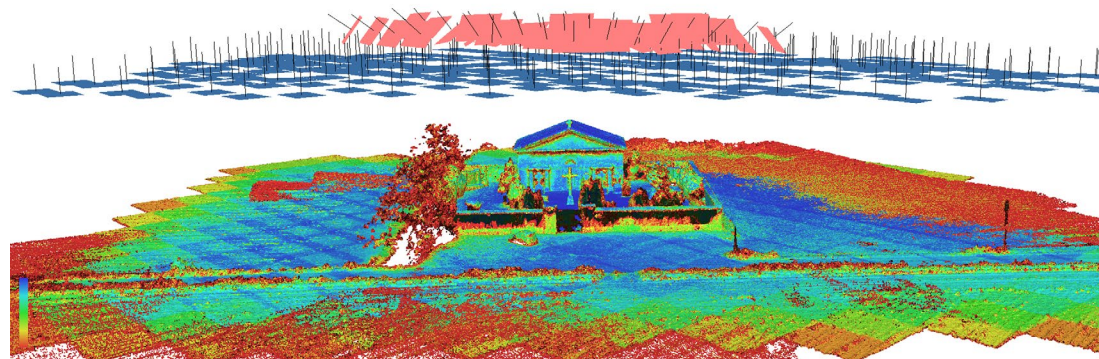

Fig. 8 - Sum of the frames of the first and second mission.

regarded as an evolution of Fast(er) R-CNN, originating from R-CNN. Despite the improvements made by this type of architecture, some problems remained. For example, significant time was still required to train the network, and the algorithm for selecting regions for object identification was not interactive.
Some of the limitations of R-CNN were improved in Fast R-CNN - proposed by the same author of R-CNN - but it was only with Faster R-CNN (Ren et al., 2016) that the area selection algorithm for object identification was itself replaced by a neural network.
The previous algorithm was in fact, slow and laborious and affected the performance of the network. This and other improvements led to the new architecture being able to perform multiple object recognition operations in less than a second, as opposed to the previous architectures that took up to 50 seconds per image.
The architectures of the networks described up to this point only allow object detection operations to be performed, as objects are identified within the images that are fed to these architectures. These networks in fact, have only two stages within them, the first, the backbone, which is responsible for producing the regions of space within which to produce the identification, and the second, which is responsible for the identification itself and the estimation of the bounding box around the identified object.

Mask R-CNN proposes an extension of the second stage, adding to the identification of the bounding box layers that take care of extracting a Region of Interest (RoI) and, consequently, a mask that estimates the segmentation of the identified object. This operation is carried out with a negligible decrease in performance compared to Faster R-CNN.

We can therefore summarize, with respect to the development of this algorithm, how the main advantages sought are: (i) greater speed, thanks to the consideration of the framing of the detected object as a regression problem, which allows for a simplified pipeline; (ii) an overall view, since the analysis on which the predictions are based is carried out considering the image in its entirety and totality; (iii) the recognition of generalized objects; (iv) the robustness of the algorithm with respect to the recognition of objects, even those of small dimensions within the image.

INTEGRATED DATA RESTITUTION METHODOLOGY

To perform object segmentation operations, the network was trained on the publicly available Common Objects in COntext (COCO) dataset (Lin et al., 2015). The COCO dataset is state of the art as far as publicly available datasets oriented towards visual machine learning operations are concerned. The dataset in fact, contains 123287 images within it with 886284 object instances with-

in the images. The advantage of using the COCO dataset is the contextualisation of the objects. The objects are in fact proposed within contexts that are useful in reducing the network overfit problem. Each image file is accompanied by another file containing: (i) the labels of the objects within it, (ii) the bounding boxes of the objects within it, (iii) the masks of the objects.

For the network training, the same values can be found in the implementation (Mask R-CNN for Object Detection and Segmentation, 2017/2022) provided by Matterport (Tomalini & Pristeri, 2022) of Mask R-CNN were used for the network architecture and its hyperparameters.

Unlike the version proposed by Matterport, in this case the network was only trained on the 'person' and 'car' classes in the dataset. Reducing the classes on which an object detection-oriented network is trained may reduce problems in identifying false positives, especially in real-world contexts such as the one examined in this contribution.

The network training operations were carried out on a machine equipped with an Nvidia 1080 Ti GPU with 12GB of VRAM, 64GB of system ram and version 35 of the Fedora Server operating system. The version of Python used for the training script and to perform the inference is 3.6.10. Details on the versions of the individual Python modules are available on the Matterport repository. An 80 / 20 split was used for training the model. The training

time is clearly influenced by other processes running on the machine and is therefore not considered relevant in this context (Fig. 9).

Validation was performed on the dataset collected for this contribution. The metric used to assess the accuracy of the network is Mean Average Precision (mAP), which is also used by the maintainers of the COCO dataset themselves. In this case, the mAP, calculated using the formula (Formula 2) was found to be 0.95. In this case, the Mean Average Precision is clearly averaged over only two classes, those used for training the model.

The measured accuracy on the test case has been found to be sufficient for achieving the desired goal which was to remove unwanted objects (e.g. a car), which the network was searching for, from the output point clouds. The masking approach also allows to just remove the unwanted object from the input pictures, minimizing the discarding of useful data. The advantage of implementing this step in the process is to mitigate the risk of having to manually correct the point clouds in the case an obstacle is present.

CONCLUSIONS

The contribution presents the development of two methodologies that aim to optimize photogrammetric acquisitions in the architectural field. The first procedure overcomes the limitation of native
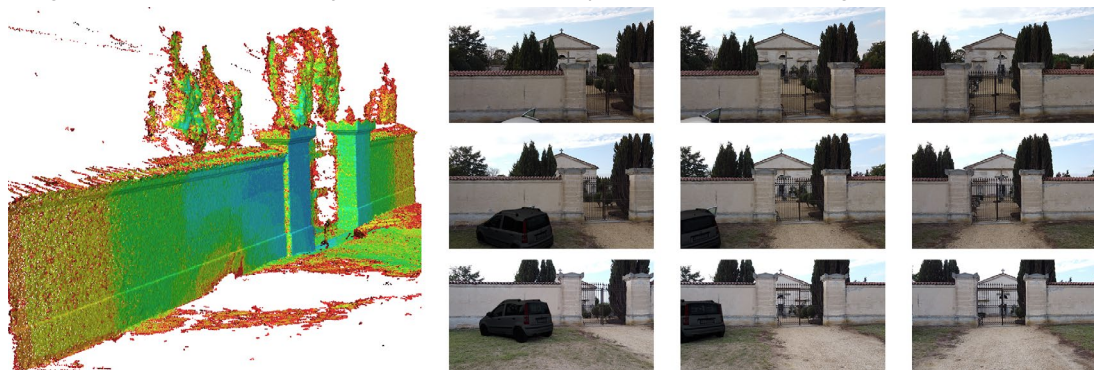

Fig. 9 - Dense cloud recalculated after automatic application of the masks calculated by the R-CNN Mask framework. The car was correctly recognized when fully visible but this was enough to get a cloud already cleared of this obstacle.

Formula 2: Mean Average Precision

$$mAP = \frac{1}{N} \sum_{i=1}^{N} APi$$

applications compatible with inoffensive UAS that are not enabled to construct specific missions for photogrammetry. The development of algorithms in the VPL environment aims to define customized paths by the operator according to specific needs. The second methodology aims to improve the photogrammetric restitution by eliminating objects that could be a source of noise or are not interested in the restitution. Object segmentation algorithms identify those classes of objects not desired within the restitution and automatically create masks that remove the object from the photogrammetric calculation. Both methodologies are in the development phase, and although they have some limitations due to a still incomplete development, they return very promising results. In the first case, the significant limitations are not software limitations but rather due to the sensors that characterize the drone; in this regard, the research group is confident in the continuous evolution of these systems that will soon, hopefully, achieve increasingly appreciable performance.

Regarding the second methodology, the algorithms used are solid and have a reference bibliography that confirms their operation. The limitation of these frameworks is intrinsically linked to the datasets with which they are loosely coupled. It is necessary to have numerous correctly metadata images to have an algorithm that works properly. During this brief experiment, we relied on free datasets that, despite the excellent results obtained, could be further implemented by increasing entropy by supplementing with further images (in this use case, it would have been useful to supplement the dataset with images of cars destined for the European market). The research team, encouraged by the results obtained, intends to continue these procedures to solve the problems encountered.

NOTE

[1] The term refers to the airspace between o-120 metres, i.e. the altitudes most frequently used by drones.

[2] The portal dedicated to UAS operators for the provision of registration, declaration, geo-awareness, remote identification and publication of geographical zone information services (definition from ENAC regulation)

[*]Author Contributions:
Although the contribution was conceived jointly,
Andrea Tomalini is author of paragraphs "introduction", "methodology for flight planning and flight" and "mission conduct and commentary";
Edoardo Pristeri is author of paragraphs "introduction to mask R-CNN and object segmentation" and "integrated data restitution methodology";
Jacopo Bono is author of paragraphs "introduction to photogrammetry survey", "regulatory background in Italy for UAS use" and "UAS used";
Conclusion is written by Andrea Tomalini, Edoardo Pristeri and Jacopo Bono.

REFERENCES

Aicardi, I., Chiabrando, F., Lingua, A.M. & Noardo, F. (2018) Recent trends in cultural heritage 3D survey: The photogrammetric computer vision approach. *Journal of culture heritage*, 32, 257-266

ARS, D. (2021, dicembre 21). *DJI Waypoint* (Spiegati per i principianti). DJI Authorized Retail Store. https://www.dji-store.it/dji-waypoint-spiegati-per-i-principianti/

Civil drones (unmanned aircraft). (s.d.). EASA. Recuperato 26 settembre 2022, da https://www.easa.europa.eu/en/domains/civil-drones

De Luca, L. (2011). *La fotomodellazione architettonica*. Palermo: Dario Flaccovio Editore.

Girshick, R., Donahue, J., Darrell, T., & Malik, J. (2014). *Rich feature hierarchies for accurate object detection and semantic segmentation* (arXiv:1311.2524). arXiv. http://arxiv.org/abs/1311.2524

He, K., Gkioxari, G., Dollár, P., & Girshick, R. (2018). *Mask R-CNN* (arXiv:1703.06870). arXiv. http://arxiv.org/abs/1703.06870

Lin, T.-Y., Maire, M., Belongie, S., Bourdev, L., Girshick, R., Hays, J., Perona, P., Ramanan, D., Zitnick, C. L., & Dollár, P. (2015). *Microsoft COCO: Common Objects in Context* (arXiv:1405.0312). arXiv. https://doi.org/10.48550/arXiv.1405.0312

Lo Brutto, M., A. Garraffa, and P. Meli. 2014. "UAV Platforms for Cultural Heritage Survey: First Results." In ISPRS Annals of Photogrammetry, Remote Sensing and Spatial Information Sciences, II-5:227–34. Copernicus GmbH.

Marin-Buzòn, C, Pèrez-Romero, A., Lopez-Castro, J.L. Jerbania, I.B., Manzano-Agugliaro, F. (2021) Photogrammetry as a New Scientific Tool in Archaeology: Worldwide Research Trends. *Sustainability*, 13, 1-27

Mask R-CNN for Object Detection and Segmentation. (2022). [Python]. Matterport, Inc. https://github.com/matterport/Mask_RCNN (Original work published 2017)

Nex, F., & Remondino, F. (2014). UAV for 3D mapping applications: A review. *Applied Geomatics*, 6(1), 1–15. https://doi.org/10.1007/s12518-013-0120-x

Ren, S., He, K., Girshick, R., & Sun, J. (2016). *Faster R-CNN: Towards Real-Time Object Detection with Region Proposal Networks* (arXiv:1506.01497). arXiv. http://arxiv.org/abs/1506.01497

THE EU DRONE POLICY. (s.d.). [Text]. European Commission - European Commission. Recuperato 26 settembre 2022, da https://ec.europa.eu/commission/press-corner/detail/en/memo_16_4123

Tomalini, A., & Pristeri, E. (2022). *Real-Time Identification of Artifacts: Synthetic Data for AI Model* (pagg. 227–234). https://doi.org/10.3280/oa-845-c216